Journal of the European Ceramic Society 20 (2000) 951–958

Bulk and grain boundary diffusion of titanium in yttria-stabilized zirconia

K. Kowalski [a,b,*], A. Bernasik [a,b], A. Sadowski [a]

[a] *University of Mining and Metallurgy, al. Mickiewicza 30, Kraków, Poland*
[b] *Surface Spectroscopy Laboratory, Joint Centre for Chemical Analysis and Structural Research, Jagellonian University and University of Mining and Metallurgy, ul. Reymonta 23, Kraków, Poland*

Received 2 June 1999; received in revised form 28 June 1999; accepted 8 August 1999

Dedicated to the memory of Professor Jan Janowski

Abstract

Bulk and grain boundary diffusion of titanium in yttria fully stabilized zirconia was studied in air in the temperature range from 1200 to 1400°C. The secondary ion mass spectrometry (SIMS) technique was used to determine the diffusion profiles in the form of mean concentration vs depth in B-type kinetic region. In order to confirm that the diffusion occurred in the chosen kinetic regime the 3-dimensional distribution of titanium was also determined. The obtained results allowed to calculate the temperature dependence of the bulk diffusion coefficient D and the grain boundary diffusion parameter $D'\delta s$. Activation energies of these processes amount to 505 and 340 kJ mol^{-1}, respectively. © 2000 Elsevier Science Ltd. All rights reserved.

Keywords: Diffusion; Grain boundaries; Titanium diffusion; ZrO_2

1. Introduction

Fully stabilized zirconia (with Ca, Y, Mg, Ce etc. as stabilisers) is one of the most technologically important ceramic materials. It is used in many types of devices which are based on its electrical, electrochemical and mechanical properties. This material is prepared by sintering at high temperatures and it usually works at elevated temperatures. In these conditions several processes involving mass transport occur, such as sintering, creep, re-crystallisation, corrosion and ageing as well as migration of dopants and impurities. These processes are mainly controlled by slow transport of cations as anion diffusion in the stabilized zirconia is several orders of magnitude higher than that of cations.[1]

The knowledge of lattice and grain boundary diffusion coefficients of cations, constitutes the main point in understanding and interpretation of the mass transport processes. Little is known, however, on the cation kinetics in zirconia, especially on the diffusion along grain boundaries. This lack of data is caused by difficulties in investigating the diffusion in ceramic materials.[2–4] The properties of polycrystalline non-metallic compounds, e.g. oxides, are highly influenced by impurities. It is rather difficult to produce dense and non-porous ceramic material of high purity and free of extended defects.

Experimental difficulties arise also from the fact that the cation diffusion in zirconia is very slow. Direct method which allows to determine the diffusion coefficients is classical radiotracer serial mechanical sectioning. However, for correct determination of the diffusion coefficients this method requires that mean penetration distance of the diffusing tracer $(Dt)^{1/2}$ (where D is bulk diffusion coefficient, t is annealing time) should be at least several micrometers. To satisfy this condition for zirconia the diffusion annealing temperatures should exceed 1700°C. Using this method, Rhodes and Carter[1] have determined the bulk diffusion coefficients of ^{45}Ca and ^{95}Zr in calcia fully stabilized zirconia in the temperature range 1700–2200°C.

In addition to this direct method some indirect experiments have also been used to evaluate the diffusion coefficients in the fully stabilized zirconia. Oishi et al.[5–7] have determined the interdiffusion coefficients in bulk and grain boundaries of Hf-Zr in the temperature range 1375–1700°C and of Ca-Zr in the range 1450–2116°C. They applied the X-ray microprobe analysis to

* Corresponding author. Tel.: +48-12-617-27-16; fax: +48-12-634-30-70.
E-mail address: kowalski@zawrat.metal.agh.edu.pl (K. Kowalski).

0955-2219/00/$ - see front matter © 2000 Elsevier Science Ltd. All rights reserved.
PII: S0955-2219(99)00212-5

determine diffusion profiles on the cross-sections of two coupled polycrystalline samples of calcia, magnesia and yttria-stabilized zirconia containing different amounts of stabilisers or Hf dopant. Creep studies[8,9] of yttria fully stabilized zirconia allowed to evaluate effective diffusion coefficients in this material at temperatures exceeding 1400°C. Mobility of Zr point defects in the yttria stabilized zirconia was studied in the range 1100–1275°C by transmission electron microscopy (TEM) observations of the shrinkage rates of small dislocation loops introduced by high temperature plastic deformation of single crystals.[10] The results of these investigations are collected in Table 1. As can be seen there are only few data on the cation diffusion in the stabilized zirconia and these data have been mostly obtained by indirect methods at very high temperatures.

The aim of this work is to determine the bulk (lattice) and grain boundary diffusion parameters of titanium in the yttria fully stabilized zirconia by applying the secondary ion mass spectrometry (SIMS) technique for the determination of diffusion profiles. This approach compared to other techniques enables the investigation of the diffusion process at much smaller penetration depths. Consequently, diffusion can be studied at lower temperatures. The diffusion profiles obtained by this method, which is analogous to the serial mechanical sectioning, permit direct determination of the bulk and grain boundary diffusion parameters.

2. Theoretical background

In this work experimental determination of the bulk and grain boundary diffusion parameters is based on the Fisher model[11] of diffusion along a single grain boundary adapted by LeClaire to the polycrystalline material.[12] The mathematical description of this model, its exact solutions given by Whipple[13] and Suzuoka[14,15] and its application for polycrystals proposed by LeClaire[12] are reviewed in detail in the book by Kaur and Gust,[16] the papers by Peterson[17] and Mischin et al.,[18] where all the original works are quoted and discussed.

In this model, grain boundary is considered as a thin slab perpendicular to the surface. Generally, three regimes of the diffusion process (or kinetics) in polycrystalline material, denoted as A, B and C, are distinguished.[11–13] The regimes are classified according to the relation between grain size g, grain boundary width δ, mean penetration distance in the bulk $(Dt)^{1/2}$ and grain boundary segregation factor s of the diffusing element. The segregation factor is defined as the ratio between grain boundary and bulk concentration of the element. For the determination of grain boundary diffusion kinetics regions B and C are the most interesting.

In the regime C, valid for $(Dt)^{1/2} << s\delta$, the transport process occurs along grain boundaries only. In this case one can calculate the grain boundary diffusion coefficient directly from the diffusion depth profile, obtained by the serial sectioning method. Unfortunately, in practice it is very difficult to perform the diffusion experiment complying with this condition because the annealing times should be extremely short and/or the temperatures rather low. Even in the case when the diffusion is very slow and the annealing time is reasonably short (at least several minutes) the investigated material should have a dense network of grain boundaries, because the tracer is located only inside the grain boundaries. Mean concentration of the tracer in the whole sample is very low. In order to increase this concentration the grains should be as small as possible. On the other hand it is very difficult to obtain non-porous ceramic material consisting of ultrafine grains. That is why the diffusion experiments are mostly made in the regime B where the conditions are much easier to satisfy.

The regime B is valid when

$$s\delta << (Dt)^{1/2} << g \tag{1}$$

This condition means that mean penetration distance in the bulk is much greater than the grain boundary width and much smaller than the grain size. In this regime three transport processes occur. The first one is direct bulk diffusion from the surface to the volume of the grains adjacent to the surface. The second one is diffusion along grain boundaries. In this case the grain boundary diffusion coefficient, traditionally denoted as D', is much greater than the bulk diffusion coefficient $D(D' >> D)$. The third process is bulk diffusion from grain boundaries toward the neighbouring grains. The mean penetration distance $(Dt)^{1/2}$ is so small that the tracer fluxes coming from different grain boundaries do not overlap.

Diffusion profile in region B, expressed as mean concentration of the tracer vs depth, consists of two parts. The first part, characterised by high slope, depends on the diffusion from the surface to the bulk of the grains. From this part it is possible to calculate the bulk diffusion coefficient using the equation, valid for the instantaneous source boundary condition (very thin layer of the deposited tracer):[11–13]

$$D = -\left(4 \cdot t \cdot \frac{\partial \ln \bar{c}}{\partial x^2}\right)^{-1}, \tag{2}$$

where $\bar{c}$ is average concentration and x is depth.

The second part of the concentration profile shows much lower slope and it represents the diffusion from

Table 1
Literature data on the diffusion in the fully stabilized zirconia

No.	System	Transport process	Method	Temperature range (°C)	Bulk diffusion $D = D_0 \times \exp(-Q/T)\,[m^2s^{-1}]$		Grain boundary diffusion $D'\delta s = D'_0\delta_0 s_0 \times \exp(-Q'/RT)\,[m^3s^{-1}]$		Ref.
					$D_0\,[m^2s^{-1}]$	$Q\,[kJ\,mol^{-1}]$	$D'_0\delta\,[m^3s^{-1}]$	$Q'\,[kJ\,mol^{-1}]$	
1.	16 mol% $CaO\text{-}ZrO_2$	^{45}Ca tracer diffusion	Mechanical sectioning	1700–2150	4.44×10^{-5}	419	–	–	1
2.	16 mol% $CaO\text{-}ZrO_2$	^{95}Zr tracer diffusion	As above	As above	3.5×10^{-6}	387	–	–	1
3.	12 mol% $CaO\text{-}ZrO_2$	As above	As above	As above	3.5×10^{-6}	387	–	–	1
4.	16 mol% $CaO\text{-}(Zr_{1-x}Hf_x)O_2$ $x_1=0.020$, $x_2=0.100$	Interdiffusion Zr-Hf	Profile obtained by X-ray microprobe	1502–2083	2.3×10^{-6}	376	9.8×10^{-14}	256	5
5.	14 mol% $MgO\text{-}(Zr_{1-x}Hf_x)O_2$ $x_1=0.020$, $x_2=0.100$	As above	As above	1680–2083	3.3×10^{-6}	381	1.2×10^{-13}	256	5
6.	16 mol% $Y_2O_3\text{-}(Zr_{1-x}Hf_x)O_2$ $x_1=0.020$, $x_2=0.100$	As above	As above	1584–2116	3.1×10^{-6}	391	1.5×10^{-12}	309	6
7.	13 mol% $CaO\text{-}ZrO_2$ 19 mol% $CaO\text{-}ZrO_2$	Interdiffusion Ca-Zr	As above	1375–1650	1.98×10^{-4}	423	2.9×10^{-7}	414	7
8.	25 mol% $Y_2O_3\text{-}ZrO_2$	Effective lattice diffusivity	Creep measurements	1400–1600	3.0×10^{-1}	564	–	–	8
9.	9.4 mol% $Y_2O_3\text{-}ZrO_2$ single crystal	Zr Vacancy diffusion	A dislocation loop annealing study	1100–1300	1.4×10^{-3}	511	–	–	10
10.	18 mol% $Y_2O_3\text{-}ZrO_2$ single crystal	As above	As above	As above	9.6×10^{-5}	511	–	–	10

grain boundaries into the grains. The product $D'\delta s$ can be calculated according to the equation:[16–18]

$$D'\delta s = 0.66 \cdot \left(-\frac{\partial \ln \bar{c}}{\partial x^{6/5}}\right)^{-5/3} \cdot \left(\frac{4D}{t}\right)^{1/2} \quad (3)$$

In region B it is not possible to find directly the grain boundary diffusion coefficient D'. This coefficient can be calculated when the grain boundary width δ and the segregation factor s are known from independent experiments. Nevertheless, the term $D'\delta s$, equal to the mass flux, is very useful because it enters several equations describing mass transport processes in solids like sintering, diffusional creep etc.

In this work the diffusion experiments were performed in the B regime.

3. Experimental

The samples of yttria stabilized zirconia (92 mol% ZrO_2–8 mol% Y_2O_3) in the form of round pellets (10 mm diameter, 2 mm thickness) were prepared by sintering the fine-grained (0.3 μm) powder compacts at 1700°C for 2 h. The powder was prepared by the co-precipitation of salt solutions ($ZrOCl_2$, YCl_3) and subsequent calcination and milling. Thus obtained polycrystalline zirconia samples were dense (density >99%) and consisted of grains with the average diameter of 15 μm. X-ray diffraction (XRD) measurements were applied to verify the crystallographic structure of the material. The investigated samples showed cubic phase only. Applying the X-ray grazing incidence (1–2°) of the primary beam, XRD measurements showed that the cubic phase at the surface was stable in the annealing experiments.

Thin films of TiO_2 were deposited on the polished surface of the samples by RF sputtering from Ti mosaic target in an Ar + 15% O_2 gas atmosphere. The sputtering rate did not exceed 2 nm/min. The as-sputtered films were amorphous. Their thickness evaluated by profilometer was about 30 nm.

The diffusional annealings were performed in air at 1200, 1250, 1350 and 1400°C for 24, 12 and 1.5 h respectively and at 1300°C for 1.5 and 6 h. For each temperature the time of annealing was chosen according to the literature data and some preliminary experiments in the conditions given by Eq. (1). The change of grain size on annealing was verified by means of scanning electron microscopy. Preliminary experiments have shown that annealing did not cause any change of grain size and/or their sintering.

The SIMS in-depth profiles were determined in a Vacuum Scientific Workshop Ltd. apparatus under the pressure less than 10^{-8} mbar. Double lens liquid metal ion beam gun (FEI Company) was used to sputter the area of about 100 μm×100 μm with Ga^+ primary ion beam of the energy 25 keV and current 2 nA. Secondary ions were detected in the Balzers quadrupole mass spectrometer. In order to avoid the undesirable edge effects only the ions coming from the central 40% of the crater area were analysed. Charging effects on sputtering were avoided by applying the electron flood gun with the energy of about 250 eV. The crater dimensions were sufficient to analyse several grains as well as grain boundaries between them. Typical SIMS crater obtained in this work is presented in Fig. 1. Depths of the craters were measured by a profilometer. They were usually in the range between 1.5 and 2 μm. One such crater profile is shown in Fig. 2. The depth inaccuracy resulting from roughness of the crater bottom is about 8%.

Diffusional profiles of titanium in the yttria stabilized zirconia were determined by the measurements of signal intensities of four isotopes: ^{48}Ti, ^{89}Y, ^{90}Zr and ^{94}Zr on sputtering.

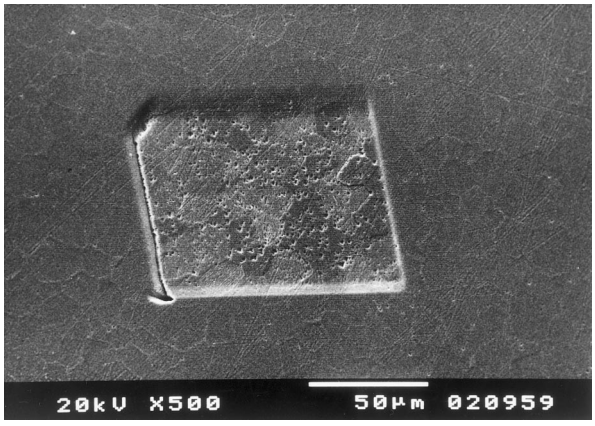

Fig 1. Micrograph of SIMS crater (depth ~1800 nm).

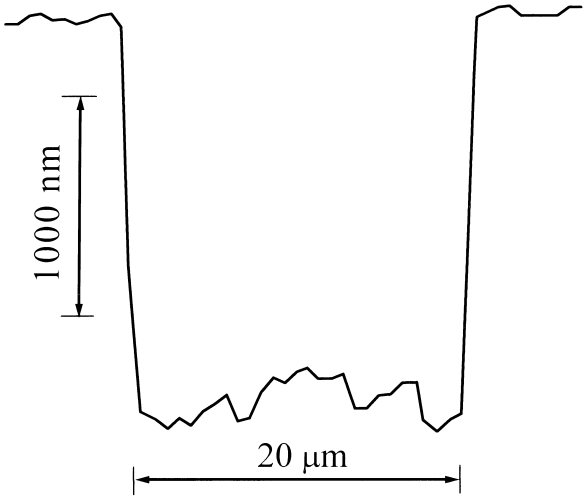

Fig 2. Profile of the SIMS crater obtained by the profilometer.

Time of sputtering to obtain correct diffusional profile was usually about 3 h. To verify the results, the measurements were repeated several times in different areas of the same sample.

The SIMS method was also applied to determine the distribution of the ^{48}Ti isotope in thin slices of material removed successively on sputtering. This allowed to obtain three dimensional distribution of titanium in the sputtered volume (3D-profiling).

4. Results and discussion

Depth profiles of titanium, yttrium and zirconium for the not annealed zirconia sample covered with a thin TiO_2 film are illustrated in Fig 3. Passing from the titania film to the bulk of yttria stabilized zirconia the Ti signal abruptly decreases to a very small value, close to the detection limit of the analyser, which means that its concentration is practically equal to zero. The intensities of signals of other isotopes remain constant when passing in depth of zirconia. If it is assumed that the sputtering rates of TiO_2 and zirconia are the same thickness of the TiO_2 film is about 30 nm. This result is in good agreement with one obtained by the profilometer. The experiment repeated in several places of the same sample showed that depth resolution in the TiO_2/zirconia interface was about 10 nm. This value is close to the resolution limit of the SIMS method and therefore it can be concluded that the polishing procedure gave very smooth surface of zirconia and the TiO_2 film was uniform.

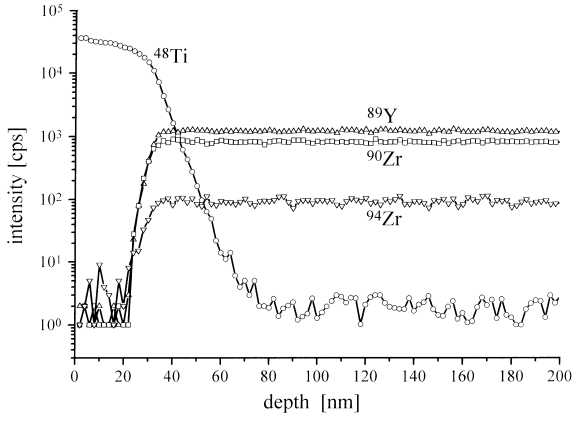

Fig 3. Depth profiles of different isotopes of the not annealed zirconia sample covered with the TiO_2 film.

The results of SIMS measurements for next mathematical operations were analysed as a function of intensity ratios: $^{48}Ti/^{90}Zr$, $^{89}Y/^{90}Zr$ and $^{94}Zr/^{90}Zr$ vs depth. This procedure allowed to avoid problems resulting from small variations of the secondary ion currents during the sputtering time. Obviously the relative intensities of signals produced by isotopes with constant concentration in the bulk of the material (this is ^{89}Y, ^{90}Zr and ^{94}Zr) should remain constant. The constant value of the ratios $^{89}Y/^{90}Zr$ and $^{94}Zr/^{90}Zr$ in the bulk of yttria stabilized zirconia was the criterion of the measurement correctness.

Typical diffusion profile is shown in Fig. 4. The dots represent experimental points and solid the Ti profile calculated according to Eqs. (2) and (3). It should be noted that the intensity ratios $^{89}Y/^{90}Zr$ and $^{94}Zr/^{90}Zr$ are constant. The diffusion profile of Ti consisted of two parts. By applying Eq. (2) to the first part of the profile and Eq. (3) to the second part, the values of the bulk diffusion coefficients D and the product $D'\delta s$ characterising the grain boundary diffusion were calculated. For calculating the grain boundary diffusion parameters $D'\delta s$ the values of D obtained from the same profile were used.

The values of D and $D'\delta s$ obtained in this work, presented in the Arrhenius plot, are shown in Fig. 5. The least square method allowed to determine the following expressions for the bulk diffusion coefficient:

$$D = 4.2(3.8)\cdot 10^{-2}\cdot \exp\left(\frac{-505(32)\,\mathrm{kJ\,mol^{-1}}}{RT}\right)\left[\mathrm{m^2\,s^{-1}}\right] \quad (4)$$

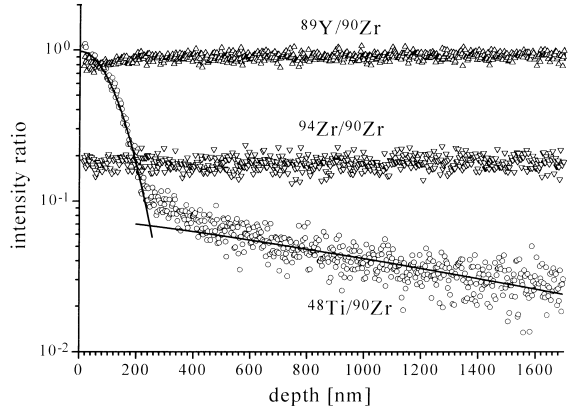

Fig 4. Diffusional depth profile obtained for the specimen annealed at 1300°C for 1.5 h.

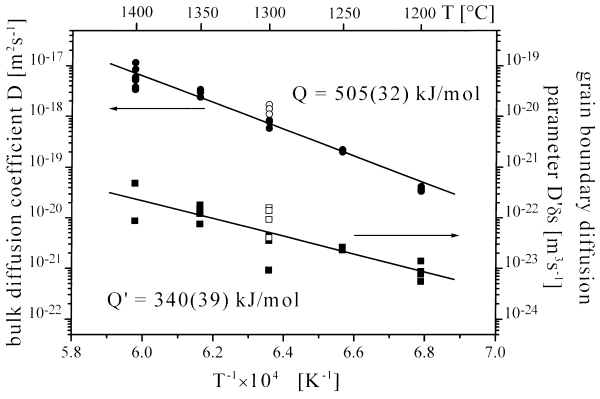

Fig 5. Arrhenius plot of the diffusion parameters obtained in this work.

where T is absolute temperature of annealing and R is gas constant, and for the grain boundary diffusion parameter

$$D'\delta s = 1.0(3.8)\cdot 10^{-11}\cdot \exp\left(\frac{-340(39)\text{kJ mol}^{-1}}{RT}\right) \times \left[\text{m}^3\,\text{s}^{-1}\right] \quad (5)$$

Values in brackets are standard deviations.

The results from different places on the sample annealed at a given temperature exhibit some scatter which designates experimental error (Fig. 5). Time of annealing had no effect on this scattering. For illustration, at the temperature of 1300°C open dots refer to the sample annealed for 1.5 h and solid dots to the sample annealed for 6 h. Taking into account the experimental error these results are in good agreement. In general,

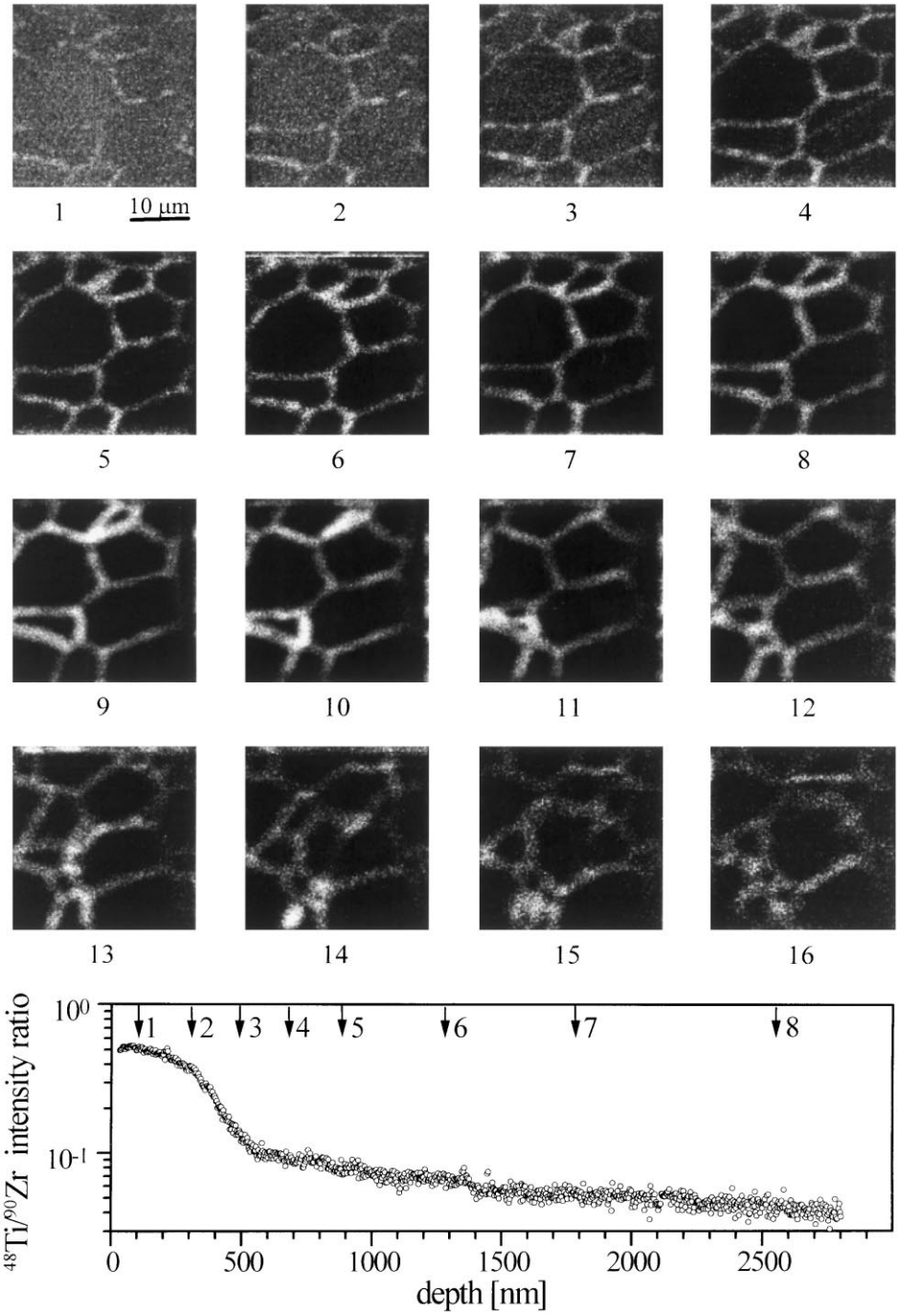

Fig 6. Distribution of titanium in thin slices parallel to the sample surface in the function of depth compared with the depth profile of the mean Ti concentration obtained for the same specimen annealed at 1400°C for 1.5 h.

results obtained for grain boundary diffusion are more scattered than those for bulk diffusion. This is quite obvious because to determine the grain boundary parameter from Eq. (3) it is necessary to use the values of D with their own errors and in this way the total error accumulates.

An important problem is to answer the question whether the mean concentration profiles obtained on sputtering really correspond to the distribution of titanium caused by the bulk and grain boundary diffusion and not by other processes or artefacts. The shape of the profiles, even if characteristic for the B-type kinetics, is not a sufficient criterion. Therefore additional SIMS measurements were performed in order to determine 3-dimensional distribution of titanium. This distribution was compared with the mean concentration profile obtained for the same sample.

Fig. 6 shows a set of 16 maps illustrating the distribution of titanium (^{48}Ti) in thin slices parallel to the surface in function of depth for the sample annealed at 1400°C for 1.5 h. Positions of the maps numbered from 1 to 8 on the depth scale are marked on the corresponding depth profile of the mean concentration of titanium. The depths of maps 9 to 16 are about 3320, 4090, 4860, 5630, 6400, 7170, 7940, 8710 nm respectively. Maps 1 to 3 correspond to the region of the first part of the profile. It can be seen that titanium is distributed uniformly inside the grains. The greater the distance from the surface, the lower the concentration of titanium inside the grains as well as network of the grain boundaries more pronounced. Map 4 is taken from the transition region and maps 5–8 correspond to the range of small slope on the profile. Here titanium is concentrated near the grain boundaries only. In this range the picture of the grain boundary network does not change from one map to another which means that the grain boundaries can be considered as perpendicular to the surface. Then the distribution of titanium on these maps is consistent with the mathematical model of the diffusion in B-type kinetic region. All diffusion profiles of the mean concentration of titanium determined in this work were taken in this range.

Maps 9–16 refer to greater depths at greater intervals. The image of grain boundary network changes from one map to another. Some grains disappear and other appear instead. It means that within this range of depth the mathematical formalism presented previously is not valid.

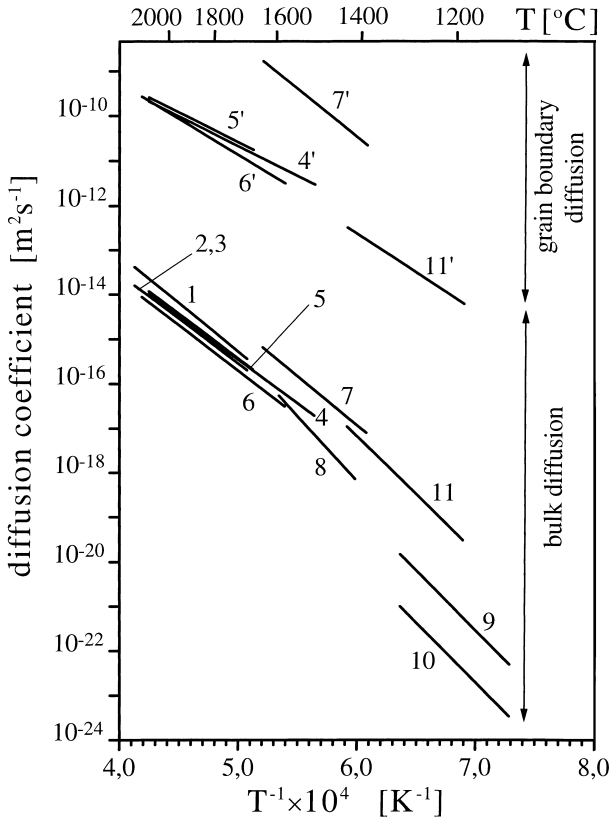

Fig 7. Bulk and grain boundary diffusion coefficients in fully stabilized zirconia obtained by different authors. The numbers of curves correspond to No. of data in column 1 in Table 1. The data marked 11 and 11′ are obtained in this work.

The results obtained in this work are compared to the literature data on the diffusion coefficients for Ca, Y and Mg -stabilized zirconia in Fig. 7. The numbers of curves correspond to the numbers of the data cited in the Table 1 (first column). ''Primed'' numbers concern the grain boundary diffusion coefficient. The data marked 11 and 11′ are determined in this work and correspond to Eqs. (4) and (5), respectively. The grain boundary diffusion coefficients D' were calculated from the experimentally determined values of $D'\delta s$ product with the assumption that the grain boundary width is close to 1 nm and the segregation factor about 1. There is little information concerning the width of grain boundaries in ceramics and its dependence on the temperature. However, the reported data[4,19,20] indicate that the above assumption is reasonable. Obviously, the segregation factor is equal to 1 for self-diffusion while for heterodiffusion it is usually different. The X-Ray Photoelectron Spectroscopy (XPS) study of the segregation of titanium in the yttria fully stabilized zirconia (to be published) showed that the segregation factor of titanium is much less than 10 in the temperature range from 1000 to 1400°C. Also the literature data[21] indicated that the segregation factor of Ti in the titania-doped yttria-stabilized zirconia was less than 2.5 at 1400°C. Consequently, the second assumption $s \approx 1$ is also justified.

The presented results indicate that the grain boundary diffusion of titanium in the yttria stabilized zirconia is much faster than the bulk diffusion. It has been found that the values of D' are about five orders of magnitude higher than the D values. The difference is in good

agreement with the data reported by Oishi et al.[5–7] for interdiffusion of Zr-Hf in the Ca and Y-stabilized zirconia and for interdiffusion of Ca-Zr in the Ca-stabilized zirconia.

The ratio of the activation energies of the grain boundary and the bulk diffusion coefficients Q'/Q was equal to 0.67 which is close to the data reported in the literature for diffusion in metals and in the majority of ceramics.[17,19] Oishi et al.[5–7] reported the value Q'/Q varying from 0.67 to 1 (see columns 8 and 10 in Table 1). When the mechanism of diffusion along the grain boundaries is the same as in the bulk the Q' value is usually lower than that of Q. This fact is generally interpreted as lowering of the activation energy of migration and/or formation of defects in grain boundaries[17,19] caused by less-packed and highly defected structure of the grain boundaries compared to the bulk. The Q'/Q ratio equal to 0.67 suggests that the diffusion mechanisms in the grain boundaries and the bulk of investigated material are not significantly different.

5. Conclusions

Results obtained in this work for the diffusion of titanium in the yttria fully stabilized zirconia in the temperature range 1200–1400°C in air could be recapitulated as follows:

1. The grain boundary diffusion is faster than the bulk diffusion by about 5 orders of magnitude.
2. The ratio of activation energies $(Q' = 340\ \mathrm{kJ\,mol^{-1}})/(Q = 505\ \mathrm{kJ\,mol^{-1}}) = 0.67$ is characteristic for metals and the majority of ceramics. This indicates that the mechanism of diffusion in grain boundaries is the same as in bulk.
3. SIMS technique enables direct determination of the diffusion parameters. The method is relatively simple and reliable especially in studying the diffusion processes in ceramic materials where diffusion distances are too small to be analysed by the radiotracer serial mechanical sectioning.

Acknowledgements

This work was supported by the Polish State Committee for Scientific Research under Grant No 7T08A 001 10 during the years 1996–1999. We thank Prof. K. Haberko and Dr. W. Pyda for providing the materials as well as Dr. M. Radecka for depositing the titania films and the profilometer measurements.

References

1. Rhodes, W. H. and Carter, R. E., Cationic self-diffusion in calcia-stabilized zirconia. *J. Am. Ceram. Soc.*, 1966, **49**(5), 244–249.
2. Atkinson, A., Diffusion along grain boundaries and dislocations in oxides, alkali halides and carbides. *Solid State Ionics*, 1984, **12**, 309–320.
3. Atkinson, A., Grain boundary diffusion — structural effects and mechanisms. *J. de Phys.*, 1985, **46**(C4), 379–390.
4. Lesage, B., Some aspects of diffusion in ceramics. *J. Phys. III France*, 1994, **4**, 1833–1850.
5. Oishi, Y., Sakka, Y. and Ando, K., Cation interdiffusion in polycrystalline fluorite-cubic solid solutions. *J. Nucl. Mater.*, 1981, **96**, 23–28.
6. Sakka, Y., Oishi, Y. and Ando, K., Zr-Hf interdiffusion in polycrystalline Y_2O_3-$(Zr+Hf)O_2$. *J. Mater. Sci.*, 1982, **17**, 3101–3105.
7. Oishi, Y. and Ichimura, H., Grain-boundary enhanced interdiffusion in polycrystalline CaO-stabilized zirconia systems. *J. Chem. Phys.*, 1979, **71**(2), 5134–5139.
8. Dimos, D. and Kohlstedt, D. L., Diffusional creep and kinetic demixing in yttria-stabilized zirconia. *J. Am. Ceram. Soc.*, 1987, **70**(8), 531–536.
9. Jimenez-Melendo, M., Dominguez-Rodriguez, A., Gomez-Garcia, D., Bravo-Leon, A. and Martinez-Fernandez, J., Cation lattice diffusion in yttria-stabilized zirconia deduced from deformation studies. *Mater. Sci. Forum*, 1987, **239–241**, 61–64.
10. Chien, F. R. and Heuer, A. H., Lattice diffusion kinetics in Y_2O_3-stabilized cubic ZrO_2 single crystals: a dislocation loop annealing study. *Phil. Mag. A*, 1996, **73**(3), 681–697.
11. Fisher, J. C., Calculation of diffusion curves for surface and grain boundary diffusion. *J. Appl. Phys.*, 1951, **22**(1), 74–77.
12. LeClaire, A. D., The analysis of grain boundary diffusion measurements. *Brit. J. Appl. Phys.*, 1963, **14**, 351–356.
13. Whipple, R. T. P., Concentration contours in grain boundary diffusion. *Phil. Mag.*, 1954, **45**, 1225–1236.
14. Suzuoka, T., Lattice and grain boundary diffusion in polycrystals, 1961. *Trans. Jap. Inst. Metals*, 1961, **2**, 25–33.
15. Suzuoka, T., Exact solutions of two ideal cases in grain boundary diffusion problem and the application to sectioning method. *J. Phys. Soc. Japan*, 1964, **19**, 839–851.
16. Kaur, I. and Gust, W., *Fundamentals of Grain and Interface Boundary Diffusion*. Ziegler Press, Stuttgart, 1988.
17. Peterson, N. L., Grain boundary diffusion in metals. *Int. Met. Rev.*, 1983, **28**(2), 65–91.
18. Mishin, Y., Herzig, C., Bernardini, J. and Gust, W., Grain boundary diffusion: fundamentals to recent developments. *Int. Met. Rev.*, 1997, **42**(4), 155–178.
19. Monty, C. and Atkinson, A., Grain-boundary mass transport in ceramic oxides. *Cryst. Latt. Def. Amorph. Mat.*, 1989, **18**, 97–111.
20. Badwal, S. P. S. and Drennan, J., Yttria-zirconia: effect of microstructure on conductivity. *J. Mater. Sci.*, 1987, **22**, 3231–3239.
21. Theunissen, G. S. A., Winnubst, A. J. A. and Burggraaf, A. J., Surface and grain boundary analysis of doped zirconia ceramics studied by AES and XPS. *J. Mater. Sci.*, 1992, **27**, 5057–5066.